

# Critical control of flooding and draining sequences on the environmental risk of Zn-contaminated riverbank sediments

Sarah F.L. Lynch<sup>1</sup> · Lesley C. Batty<sup>1</sup> · Patrick Byrne<sup>2</sup>

Received: 31 August 2016 / Accepted: 25 December 2016 / Published online: 13 January 2017  
© The Author(s) 2017. This article is published with open access at Springerlink.com

## Abstract

**Purpose** Diffuse pollution emanating from metal mining-impacted sediment could serve as a barrier to achieving European Union Water Framework Directive and US Clean Water Act requirements. UK climate projections (UKCP09) predict increases in *rainfall* and *aridity* that will influence river stage alternately exposing and submersing contaminated riverbank sediment. Research focuses on the environmental contaminant dissolved Zn and investigates patterns of release, key geochemical mechanisms controlling Zn mobilisation and the environmental risk of sediment subjected to these perturbations. **Materials and methods** Using two laboratory mesocosm experiments, metal mining-contaminated sediment was subjected to alternate wet and dry sequences of different duration and frequency. The first experiment was run to determine the influence of submersion and exposure of contaminated sediment on releases of Zn and to establish environmental risk. The second experiment utilised diffusional equilibration in thin film (DET) to observe the patterns of Zn release, with depth, in the sediment. Pore water chemical analysis at the sediment-water interface enabled elucidation of key geochemical mechanisms of control of Zn mobilisation.

**Results and discussion** Patterns of Zn release were found to be different, depending on the length of wet and dry period. High concentrations of dissolved Zn were released at the start of a flood for runs with longer dry periods. A buildup of soluble Zn sulphate minerals over long dry periods followed by dissolution on first flood wetting was a key geochemical mechanism controlling Zn release. For longer wet runs, increases in dissolved Mn and Zn were observed over the flood period. Key geochemical mechanisms controlling Zn mobilisation for these runs were: (i) reductive dissolution of Mn (hydr)oxides and release of partitioned Zn over prolonged flood periods followed by (ii) oxidation and precipitation of Mn (hydr)oxides and sorption of Zn on exposure to atmospheric conditions.

**Conclusions** Mesocosm experiments were a first step in understanding the effects of UK climate projections on the riverbank environment. Contaminated sediment was found to pose a significant environmental risk in response to hydrological perturbations. The ‘transient’ nature of dissolved Zn release could make identifying the exact sources of pollution a challenge; therefore, further field studies are advised to monitor contaminant releases under a range of hydrological conditions and account for complex hydrology at mining sites.

Responsible editor: Marcel van der Perk

**Electronic supplementary material** The online version of this article (doi:10.1007/s11368-016-1646-4) contains supplementary material, which is available to authorized users.

✉ Sarah F.L. Lynch  
slynch\_007@hotmail.com

<sup>1</sup> University of Birmingham, Edgbaston, Birmingham B15 2TT, UK

<sup>2</sup> Liverpool John Moores University, Byrom Street, Liverpool L3 3AF, UK

**Keywords** Geochemistry · Metal pollutant · Redox potential · Riverbank

## 1 Introduction

Metal-polluted river catchments are a legacy arising from historical metal mining, mineral processing, and dumping of waste along water courses throughout the world (Macklin et al. 2006; Zhang et al. 2012). Although most mines in the UK have now closed and active mining and dumping of waste

has ceased, mining pollution arising from impacted catchments still contributes tonnes of metals to freshwater and marine environments annually (Environment Agency 2012a; Mayes et al. 2013). Point sources of pollution from adits and shafts were traditionally the focus for management and remediation approaches (Younger 1998a; Laine 1999; Younger 2000). However, there is now a greater emphasis on dealing with contamination from diffuse sources, the regulatory driver being the EU Water Framework Directive 2000/60/EC that requires management of water quality at a catchment scale delivered through the River Basin management Plans (RBMP) (Collins et al. 2012).

Zinc is a major trace metal contaminant, resulting from mining activities globally and is a worldwide environmental health concern (Zhang et al. 2012). In UK mining regions, this element is reported as the most commonly encountered trace metal in surface waters with many river systems showing evidence of chronic Zn contamination (Bird et al. 2010; Gozzard et al. 2011; Byrne et al. 2013; Foulds et al. 2014). Although Zn is essential to humans and plants, at high concentrations, it has been found to detrimentally affect macroinvertebrate community structure and function (Montserrat 2010; Gerhardt et al. 2004), contribute to fish mortalities (particularly sensitive salmonid sp.) (Fuge et al. 1991; Environment Agency, 2008a) and cause phytotoxic effects and riverbank instability (Environment Agency 2008b). Zinc is listed in the European Community (EC) Dangerous Substances Directive (76/464/EEC) because of its known toxic effects. On a national level, Zn is listed as a ‘River Basin Specific Pollutant’ (DEFRA 2014), as it can have a “harmful effect on biological quality” and may be “discharged to water in significant quantities” (UKTAG, 2008). In mining-impacted catchments, Zn is introduced into the environment when sulphide minerals such as sphalerite (ZnS) or (less commonly) wurtzite (Zn,Fe)S is brought to the surface and exposed to atmospheric conditions. Oxidation of Zn sulphide minerals can release high concentrations of Zn and sulphate into river systems. Zinc is highly mobile due to its hydrolytic stability in weakly acid solutions (Smith 1999; Lee et al. 2002) and the high solubility of many Zn sulphate minerals. As a result, it can be transported downstream over large distances as a solute. Chemical, morphological and hydrological changes within rivers will allow sorption and enrichment of Zn solid phases in riverbed and bank sediment and overbank on floodplain soils (Dennis et al. 2003; Dennis et al. 2009; Foulds et al. 2014). During high flow events, contaminated sediment can be eroded from riverbanks and floodplains and re-introduce particulate forms of Zn back into the river channel (Dennis et al. 2003; Young et al. 2007). However, more bioavailable, dissolved Zn can be re-introduced where river stage

variability and riverbank inundation results in changes in redox potential and drying of sediment (Buckby et al. 2003; Du Laing et al. 2009; Lynch et al. 2014).

UK climate projections (UKCP09) indicate an increase in the amount and intensity of rainfall, particularly in winter; as a result, peak river flow in Wales is projected to increase by 13% by 2020, 20.8% by 2050 and 27.6% by 2080 for medium emission (P50) scenarios. As a consequence, river flooding would be expected to increase in frequency (DEFRA 2012a) and duration. UK climate projections also indicate a shift towards aridity by 2020. Summer river flows are expected to decline, and Q95 (flow that is exceeded 95% of the time) may reduce by 26% by 2050 and 35% by 2080 in western Wales using medium emission (P50) scenarios (DEFRA 2012b) that could increase the length of antecedent dry period along riverbanks. As discussed in a previous paper by the current authors (Lynch et al. 2014), we hypothesised that flooding and drought brought about by future climate change will cause changes in river stage that will alternately expose and submerge riverbank sediment over varying temporal scales, alter redox potential conditions and pH and influence the mobilisation of trace metal contaminants. In mining-impacted catchments, Zn is often partitioned with Fe, Mn hydroxides (Desbarats and Dirom 2007; Du Laing et al. 2009) and sulphur-bearing minerals (Carroll et al. 1998) in the sediment. As these minerals are sensitive to redox potential and pH changes, they will undergo dissolution and precipitation reactions in response that will control Zn mobilisation. Moreover, the laying down of freshly precipitated mineral forms may increase the reactivity of minerals, potentially intensifying subsequent releases of trace metal contaminants. Previous studies have investigated the effects of alternately flooding and drying contaminated soils for different frequencies and durations on the mobilisation of Zn (Shaheen et al. 2014; Du Laing et al. 2007). However, this study is unique in that laboratory mesocosm experiments were carried out on severely metal-contaminated coarse-grained riverbank sediment, a legacy of historical mining activities. We investigate the geochemical mechanisms of Zn mobilisation in surface and pore water in response to flooding and drought sequences of different duration and frequency and utilise diffusional equilibration in thin film (DET) analysis to understand the co-distribution of Zn and Mn with depth in the sediment.

To establish the environmental risk, metal-contaminated sediment may pose in the face of future UK climate projections, this paper examines the results of two laboratory mesocosm experiments. The objectives of the study are: (1) to determine if alternately wetting and drying contaminated sediment for different durations and frequencies influences the mobilisation of dissolved Zn; (2) to identify patterns of Zn

release, with depth, in the sediment; (3) to elucidate key geochemical processes controlling the mobilisation of Zn; and (4) to assess the environmental risk the sediment poses in response to these perturbations.

## 2 Methods

### 2.1 Sediment sample site

The sample site at Cwmystwyth (SN799743) is located in central Wales at an elevation of 250 m above sea level (ASL). The mine site is drained by the Afon Ystwyth River which runs from east to west and drains into the Irish Sea at Aberystwyth (approximately 25 km northeast of Cwmystwyth). The main metalliferous vein runs parallel with the river to the north of the sample site with many old mining adits and shafts located to the east (Hughes, 1981). The north side of the river is marked by spoil heaps rising to 500 m ASL and on the south side grass banks, used primarily for grazing, rise steeply to 450 m ASL. Mining was ceased at Cwmystwyth in 1921 (Bick 1976). However, there is evidence of mining activity dating back to the Bronze Age, with peak mining occurring in the nineteenth century. The main ores mined were galena (PbS), sphalerite (ZnS) and chalcopyrite (CuFeS<sub>2</sub>), although no chalcopyrite is recorded as having been raised since 1845 and very little has been found in waste heaps (Hughes 1981). Ore veins were hosted in quartz-rich rocks. The country rock dates from the Silurian period with alternating bedrock of hard coarse sandstones and shales that form the upper Llandovery Series (British Geological Survey 2007). Rivers that rise on this type of geology have been described as ‘Base Poor’ having a low alkalinity, so it is less able to buffer acidic inputs (Natural Resources Wales 2004). The bedrock is impermeable and generally without groundwater, except at shallow depth. Superficial deposits along the river are flints, sand and silt (Centre for Ecology and Hydrology 2015).

### 2.2 Rainfall and river flow characteristics

Standard-period average annual rainfall (SAAR) for years 1981–2010 is 1856.5 mm for Cwmystwyth climate station (grid reference SN790737). This is high compared to UK SAAR for the same period (1154 mm) (MET Office 2016). Daily flow shows a highly variable pattern at the gauging station (grid reference SN790737) <1 km downstream from the sample site (Fig. 1). Generally, flow rises and recedes quickly; however, extended periods (greater than a week) of flow well above the mean value (1.989 m<sup>3</sup>/s) (leading to riverbank and floodplain inundation) and extended periods well below the mean value (leading to drainage and exposure of riverbank and floodplain) are common (Centre for Ecology

and Hydrology 2015). Changes in river flow are known to cause a rise and fall in river stage that can influence patterns of hyporheic exchange flow (the hyporheic zone is a zone of surface and subsurface/groundwater mixing that can encompass the riverbed and riverbanks) (Byrne et al. 2013).

### 2.3 Sediment collection

Sediment was collected on two occasions, July 2012 and December 2013, for analysis in two separate mesocosm treatments. Visual inspection of the northern riverbank indicated that sediment was made up of predominantly sandy gravel interspersed with some finer silt particles and larger pebbles and boulders. The sediment samples were collected from the north bank of the river at the same site, but different locations. On the first visit, sediment was taken from waste piles running along the side of the river channel. On the second visit, the sediment collected was closer to the active channel, below the waste piles and on a subsurface lateral flow path. A stainless steel shovel was used to collect sediment from the top 10 cm.

### 2.4 Laboratory analysis

#### 2.4.1 Mesocosm experiments

Two mesocosm experiments were conducted in order to meet the objectives. The first experiment was run to determine the effect alternately wetting and drying contaminated sediment for different durations and frequencies had on the release of dissolved Zn and establish whether the sediment posed an environmental risk. The second experiment concentrated on key contaminating runs from experiment 1 and utilised a passive pore water sampling technique, diffusive equilibrium in thin film (DET), to investigate patterns of dissolved Zn release, with depth, in the sediment. A combination of pore water (‘Trace metal and anion analysis’ and ‘Alkalinity and inorganic carbon analysis (water and sediments)’) and DET (section ‘Diffusional equilibration in thin film (DET) analysis’) analysis from both runs allowed the elucidation of key geochemical mechanisms of Zn mobilisation.

Mesocosms were created using unplasticized polyvinyl chloride (uPVC) drain pipe. Plain end caps (Clarks Drain) were fitted to the bottom, and holes (2.5 cm diameter) were drilled into the side of the drain pipe at the bottom (24 cm below sediment surface). Siphon tube taps were attached to polytetrafluoroethylene (PTFE) tubes and fitted into the holes. Evo-Stik waterproof sealant was added around the joints on the outside only. The sediment was homogenised by hand and then packed into each mesocosm to a depth of 24 cm using a plastic trowel (Fig. 2).

An extended experimental timeframe for each column of 20 days at field capacity, to equilibrate the sediment, followed by a maximum of 11 weeks treatment period promoted the

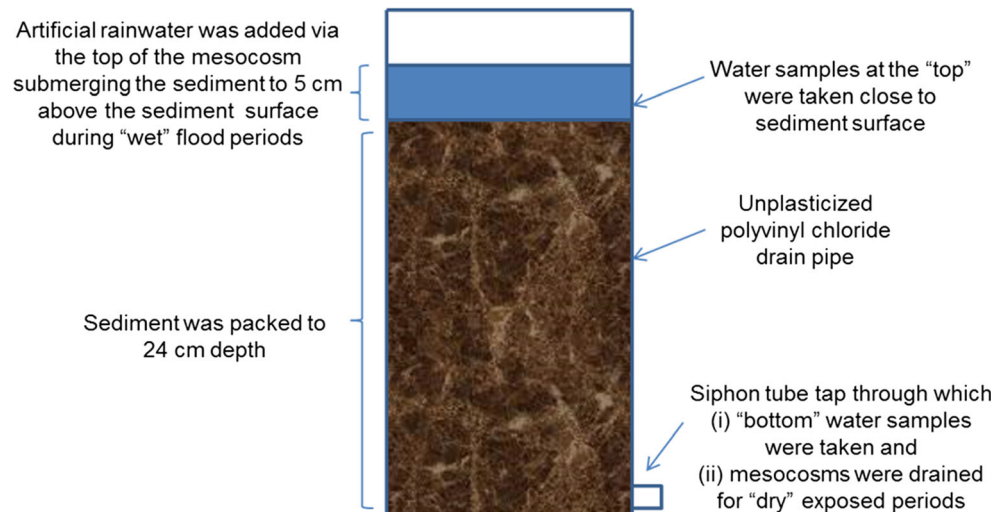


**Fig. 1** Location of sample site, grid reference SN799743 (denoted by a *star*) at the Cwmystwyth abandoned mine complex in the River Ystwyth catchment in mid-Wales (*inset*)

removal of any artefacts and allowed time for systems to settle into a steady pattern. Artificial rainwater (ARW) was created based on Plynlimon rainwater chemistry (pH 4.9–5.2) found in the uplands of mid-Wales (Neal et al. 2001). For field capacity, twice a week, 500 ml of ARW was added via the top of the mesocosm until water percolated through the bottom tap (Fig. 2). Following field capacity, mesocosms were divided into seven different treatments. Five were variable wet and dry runs and two constant controls. The Cwmystwyth gauged

daily flow (grid reference SN790737), taken from the UK National River Flow Archive (Centre for Ecology and Hydrology 2015), provided guidance regarding the length of time riverbank sediment may be exposed to atmosphere or submerged (section ‘Rainfall and river flow characteristics’). Variable runs were designed to include longer wet runs, longer dry runs and wet and dry run of same duration and frequency. Control runs were non-variable and either constant wet (flood) or unsaturated and oxidised (field capacity). This allowed a

**Fig. 2** Outline of mesocosm including sampling points





comparison between variable and non-variable wet and dry runs. Constant flood and field capacity were sampled every week. Variable run samples were taken only at the start and end of a wet period. Runs were: 1 week wet followed by 1 week dry (1wwet), 1 week wet followed by 2 weeks dry (2wdry), 1 week wet followed by 3 weeks dry (3wdry), 2 weeks wet followed by 1 week dry (2wwet), 3 weeks wet followed by 1 week dry (3wwet), Flood (Flood) and field capacity (F/C)

At the start of a flood, ARW was added completely submerging the sediment up to 5 cm above the sediment level to simulate ‘wet’ flood conditions (Du Laing et al. 2007). Water was left for 2–3 h to allow water to percolate into pore spaces and for contact time between sediment and pore water. Water samples were taken from the top using a plastic syringe and from the bottom via the tap, in that order to avoid mixing between levels and filtered through a 0.45- $\mu\text{m}$  PTFE syringe filter into two metal-free 60 ml centrifuge tubes. One sample was acidified with nitric acid ( $\text{HNO}_3$ )  $<\text{pH}$  2 for metal analysis. The other was frozen ( $-20^\circ\text{C}$ ) for subsequent anion analysis. A Hanna Combo pH/EC and temperature hand held stick meter model No 98129, recorded pH, conductivity and temperature for each sample. An Aquaread Aquameter multiparameter water quality probe was used to measure dissolved oxygen (DO) and redox potential (ORP) (2nd mesocosm experiment only). The ORP reference electrode was type 3MPK1 AgCl, and ORP readings were converted to the hydrogen scale (Eh) as instructed by Aquaread. After sampling, flood levels were kept at 5 cm above sediment level by topping up with ARW. Mesocosms were then left ‘wet’, with the taps closed, for the allotted timeframe. At the end of a wet period, the above sample methodology was repeated and any pore water remaining in the mesocosm after sampling was drained out via the bottom tap into a bucket and discarded. Mesocosms were then left ‘dry’ for the allotted timeframe. For field capacity, ARW was allowed to percolate through the mesocosm and collected at the bottom sampling point. Flood and field capacity samples were collected at the same time as the variable run samples.

#### 2.4.2 Trace metal and anion analysis

Flame atomic absorption spectroscopy (FAAS) (Perkin Elmer Analyst 300) was used to measure Fe, Mn, Zn, Ca, Ni, Cu ( $\text{mg l}^{-1}$ ) in filtered pore water samples from the 1st mesocosm experiment. Detection limits were: Ca, 0.06; Fe, 0.03; Cu, 0.01; Mn, 0.01; Zn, 0.02 and Ni, 0.01 ( $\text{mg l}^{-1}$ ). Inductively coupled plasma with optical emission spectroscopy (ICP/OES) (iCAP 6500 Duo) instrument was used to measure dissolved Fe, Mn and Zn in filtered pore water samples of the 2nd mesocosm experiment. Detection limits were: Fe, 5; Mn, 1; Zn, 5 ( $\mu\text{g l}^{-1}$ ). Ion chromatography (Dionex ICS2000) was used to measure dissolved sulphate, nitrate, chloride and

phosphate in pore water samples of the 1st mesocosm experiment and the 2nd mesocosm experiment. Detection limits were: sulphate, 0.07; nitrate, 0.04; chloride, 0.06; phosphate, 0.06 ( $\text{mg l}^{-1}$ ). Flame photometer BWB technologies were used for detection of Na, K and Ca in filtered pore water of the 2nd mesocosm experiment. For all analyses, quality control standards and blanks were used throughout. The results were considered acceptable if the data were within 5% of the expected concentration.

#### 2.4.3 Alkalinity and inorganic carbon analysis (water and sediments)

Unfiltered water samples from both mesocosm treatment runs were analysed for alkalinity (as calcium carbonate) using the standard operating procedure for Great Lakes National Program office total alkalinity titration method (United States Environmental Protection Agency 1992). Filtered pore water samples were tested for total carbon (TC) and non-purgeable organic carbon (NPOC) using a carbon analyser (Shimadzu TOC-V CSN). Inorganic Carbon = Total Carbon – Non Purgeable Organic carbon. For non-purgeable organic carbon, the sample was first acidified to pH 2 to transform inorganic carbon to  $\text{CO}_2$ . The  $\text{CO}_2$  was removed via sparging with a carrier gas. During this process, some purgeable organic carbon (benzene toluene cyclohexane and chloroform) may be partly removed, although there tends to be negligible amounts of these in surface water samples. The remaining organic carbon is ‘non-purgeable’ and is measured, as mg (of carbon) per litre of water, through  $\text{CO}_2$  detection in the analyser using a non-dispersive infrared (NDIR) detector. Standards and blanks were used throughout. The results were considered acceptable if within 5% of the expected concentration. Sediment collected for the 2nd mesocosm experiment was analysed for total organic carbon (TOC) and inorganic (IC) using a separate solid sample module of the Shimadzu instrument (SSM 5000A). A subsample of sieved (2 mm) sediment was weighed (no greater than 50 mg) and oven dried at  $140^\circ\text{C}$  for 24 h. The results provided % TC and % TIC that allowed % TOC to be calculated:  $\text{TOC} = \text{TC} - \text{TIC}$  (Shimadzu Scientific Instruments 2014).

#### 2.4.4 Statistical analysis

All calculations were performed using SPSS 20.0. Statistical tests revealed the data was not normally distributed; therefore, significant differences in pore water data were identified through non-parametric Wilcoxon rank sum test. Relationships between Zn and pore water variables were determined using Spearman’s rho 2-tailed non-directional tests. Simple regression analysis was carried out on logged Zn data and sample week (time) to assess whether there was a

significant increase in concentration of dissolved Zn at the end of a flood over treatment periods.

To determine key factors linked to the mobilisation of dissolved Zn for selected variable runs at the bottom of the mesocosms, principal component analysis (PCA) was carried out. Data was assessed to ensure (i) that underlying variables correlated (Bartlett's test of sphericity) and (ii) sampling adequacy (Kaiser-Meyer-Olkin). Factor rotation was chosen based on whether the factors (principal components, PC) were thought to be unrelated (orthogonal) or related (oblique). The importance of a principal component with regard to explaining the percentage variance of the data can be assessed from the eigenvalue. As recommended by Kaiser (1960), all principal components with eigenvalues greater than 1 were retained (Field 2009). A score was calculated for each observation and for each PC. The scores were mapped on a biplot, where the two selected PCs were the  $x$  and  $y$  axis. High variable loadings for each PC were indicated on this bi-plot (Field 2009). This allowed some indication as to what each PC might represent, how that linked to the sediment conditions created through wetting and drying and ultimately how that influenced dissolved Zn concentrations.

#### 2.4.5 PHREEQC (*Ph-redox-equilibrium in 'C'*)

The geochemical computer program PHREEQC was used for speciation and saturation index (SI) calculations using the WATEQ4F.dat database distributed with the PHREEQC program. The saturation state of Zn minerals was calculated using input data derived from pore water measurements for selected runs. Data was considered acceptable if charge balance ( $\leq 5\%$ ).

#### 2.4.6 Diffusional equilibration in thin film analysis

DET analysis was carried out in the second mesocosm experiment to measure the interaction of solutes at a higher spatial resolution (cm scale) than could be achieved through bulk pore water analysis. It was hoped this would (i) further corroborate the results obtained through pore water analysis; (ii) minimise oxidation, precipitation and sorption of redox sensitive solutes that could occur due to exposure to atmospheric conditions; and (iii) provide information regarding the co-distribution of solutes at a higher spatial scale to identify the mechanisms of dissolved Zn release that may have been missed through bulk pore water analysis. To allow time for the wet and dry sequences to become established and so measure differences in element release as a result of that wet and dry sequence, the flood period chosen for analysis was towards the end of each treatment period. DET probes (DGT Research Ltd.) were refrigerated in a sealed plastic bag with a few drops of 0.01 M NaCl until use. At the start of a flood, a stainless steel trowel was used to create a hole in the sediment in order to deploy the probe vertically into the mesocosm. A

deoxygenated DET probe was transferred to the mesocosm, allowing only a few seconds for the transfer (to minimise contact with the air). Probes were left in sediment to equilibrate for 72 h. This deployment time is thought to be sufficient for sediment to collapse around the probe, redox potential conditions to become re-established and for full equilibration to be achieved (Ullah et al. 2014). Probes were inserted for 72 h at the start of a flood and 72 h prior to the end of a flood. On removal, the gel was cut into 1 cm slices, and the method for gel cutting, storage and analysis was that used by Ullah et al. (2014) and Byrne et al. (2014). For ICP/OES analysis, the samples were diluted 1:10 with DIW. The dilution factor based on the volume of DET strip diluted in 1 ml nitric acid (as carried out by Ullah et al. 2012, 2014) with a further dilution  $\times 10$  with DIW was ( $\times 56$ ). A blank DET probe underwent all analyses except deployment. Concentrations of Fe, Mn, Zn in 10 blank DET samples were below detection. Analytical accuracy of repeat control standards was  $<5\%$ .

### 3 Results

Pore and surface water bicarbonate concentrations were undetectable. Inorganic carbon (IC) in the sediment was below detection both prior to treatment and at the end of the run. Average NPOC analysis was  $1.4 \text{ mg l}^{-1}$  ( $+0.14$ ). Based on other literature values (Meybeck 1982), this range was low medium. Ni and Cu were below detection ( $\leq 0.01 \text{ mg l}^{-1}$ ). Pore water remained slightly acidic (5.3, range 4.8–5.8) (1st mesocosm experiment), (5.7, range 5.1–5.8) (2nd mesocosm experiment), throughout the treatment periods for all runs (Tables 1 and 2).

DO and redox potential measurements taken in the 2nd mesocosm experiment showed conditions were found to be oxic  $\sim 99.5\%$  DO, Eh 494 mV, at the top of the mesocosm. DO declined to as low as 12% at the end of a flood period at the bottom of the mesocosm. The lowest redox potential measurements were taken for the 3 week wet and flood run at the bottom of the mesocosms. For these runs, a marked increase in dissolved Mn at the end of a flood was observed and dissolved Fe was measured in some cases (Table 2).

#### 3.1 Dissolved Zn in pore waters

Average concentrations of dissolved Zn at the end of a flood were found to be higher for all runs at the bottom of the mesocosms compared to the top. In the 1st mesocosm experiment, the highest average concentration was measured for the 3wdry run at the bottom of the mesocosm ( $26.8 \pm 2.9 \text{ mg l}^{-1}$ ). The lowest average concentration was for the unsaturated field capacity run ( $7.7 \pm 0.4 \text{ mg l}^{-1}$ ) (Table 1). In the 2nd mesocosm experiment, the highest average concentrations were measured for the 3wdry run at the bottom ( $61.1 \pm 6.8 \text{ mg l}^{-1}$ ),

**Table 1** 1st mesocosm experiment. Mean and range (in parenthesis) of dissolved (<0.45 µm) metals (mg l<sup>-1</sup>), pH, \*Conductivity (µS/cm), Temperature (°C) at the end of a flood, by run, Top (T) and Bottom (B) of the mesocosm. Key average values (bold and underlined), n = #

Run	1wwet (T)	1wwet (B)	2wdry (T)	2wdry (B)	3wdry (T)	3wdry (B)	2wwet (T)	2wwet (B)	3wwet (T)	3wwet (B)	Flood (T)	Flood (B)	F/C (B)
Location	n = 18	n = 18	n = 12	n = 12	n = 9	n = 9	n = 12	n = 12	n = 9	n = 9	n = 33	n = 33	n = 33
pH	5.2	5.3	5.1	5.2	5.1	5.2	5.1	5.3	5.2	5.4	5.3	5.5	5.2
(Range)	(5–5.6)	(5.1–5.5)	(5–5.3)	(5.1–5.5)	(4.8–5.3)	(5–5.3)	(4.9–5.4)	(5.1–5.5)	(4.9–5.7)	(5.2–5.7)	(5–5.8)	(5–5.7)	(5.1–5.4)
Temp °C	22.3	23.1	22.3	23.0	23.0	23.8	22.6	23.3	22.0	22.7	22.4	23.1	22.9
(Range)	(20.9–24.2)	(21.9–24.8)	(21.2–23.3)	(21.7–23.9)	(21.4–24.4)	(22.3–25.1)	(20.4–24.5)	(20.9–25.1)	(21.4–22.6)	(22.1–23.2)	(19.9–24.5)	(29.9–25)	(21–25)
*Cond	110.6	183.2	100.2	188.4	110.9	208.3	134.2	208.1	156.4	230.4	105.8	248.6	77.9
(Range)	(87–144)	(155–204)	(88–116)	(152–214)	(94–136)	(164–250)	(107–156)	(188–224)	(146–169)	(218–264)	(46–126)	(140–339)	(50–130)
Fe	0.0	0.4	0.0	0.6	0.0	0.2	0.0	3.0	0.0	6.0	0.0	8.9	0.0
(Range)	(0–0.1)	(0–1.7)	(0–0.2)	(0–1.6)	(0–0.8)	(0–0.8)	(0–0.8)	(2.2–3.9)	(0–0.5)	(3.6–10)	(0–0.5)	(0–27.7)	(0–0.5)
Mn	0.2	1.6	0.2	1.6	0.2	1.4	0.3	5.3	1.5	7.7	0.5	9.6	0.4
(Range)	(0.1–0.4)	(1.2–1.8)	(0.1–0.2)	(1.1–2.2)	(0.1–0.3)	(0.6–2.9)	(0–0.7)	(3.5–6.4)	(0.7–3.1)	(6.7–9.6)	(0–1.3)	(0.4–16.6)	(0–1)
Zn	11.2	20.7	8.3	21.8	11.2	<u>26.8</u>	15.8	21.4	15.5	18.8	10.0	17.5	<u>7.7</u>
(Range)	(3.8–20.4)	(13.8–25.2)	(4.3–12.9)	(13.3–29.8)	(6.2–18.2)	(15.2–40.5)	(8.3–23.8)	(14.9–24.9)	(10.6–18.6)	(15.5–22.6)	(1.5–15.8)	(14.2–21.4)	(3.3–13.3)
Ca	2.4	3.9	1.7	3.4	2.1	4.1	2.3	3.9	3.3	4.2	2.6	4.5	1.9
(Range)	(1.7–3.4)	(2.6–5)	(1.4–2.1)	(2.1–4.5)	(1.9–2.9)	(2.7–5.9)	(1.6–2.6)	(2.6–5)	(2.8–3.8)	(3.9–4.7)	(1.5–3.6)	(2.8–6.8)	(1.3–2.8)
NO <sub>3</sub> <sup>-</sup>	2.3	0.5	3.3	2.6	4.1	2.5	1.9	0.0	1.5	0.0	1.4	0.6	2.3
(Range)	(0–5.7)	(0–1.5)	(2–4.9)	(0–4.8)	(2.6–5.7)	(0–6)	(0.9–3)	0.0	(0–3.2)	0.0	(0–4.2)	(0–8.7)	(0.7–4.2)
Cl <sup>-</sup>	1.5	1.2	1.5	1.3	2.3	1.9	2.0	1.3	2.0	1.3	2.0	2.0	1.8
(Range)	(0.3–2.9)	(0–2.5)	(0.9–2.8)	(0.8–2.4)	(1.6–3.2)	(1.3–2.7)	(0.9–3.1)	(0.5–2.2)	(0.9–2.5)	(0.7–1.9)	(1.1–3)	(0.8–3.9)	(0–17.8)
SO <sub>4</sub> <sup>2-</sup>	38.9	71.2	44.5	84.1	42.7	87.9	48.6	82.9	61.8	95.0	46.5	119.7	36.2
(Range)	(10.8–65)	(60.2–100.8)	(25.3–90.9)	(57.3–142.8)	(25.4–63.3)	(61.2–129.5)	(34.7–63.4)	(65.3–94.2)	(47.2–85)	(79.6–121.2)	(13.5–106.4)	(47.6–277.7)	(16.9–90.5)

‘n’ relates to number of samples taken at the end of a flood period. The ‘n’ varied between runs because certain runs had more flood periods than others over the treatment period. Includes replicates

**Table 2** Second mesocosm experiment. Mean and range (in parenthesis) of dissolved (<0.45 µm) metals (mg l<sup>-1</sup>), pH, \*Conductivity (µS/cm), Temperature (°C), DOC (%), TIC (mg l<sup>-1</sup>) at the end of a flood, by run, Top (T) and Bottom (B) of the mesocosm, key average values (bold and underlined), n = #

	1wwet (T)	1wwet (B)	3wdry (T)	3wdry (B)	3wwet (T)	3wwet (B)	flood (T)	Flood (B)
	<i>n</i> = 5	<i>n</i> = 5	<i>n</i> = 3	<i>n</i> = 3	<i>n</i> = 3	<i>n</i> = 3	<i>n</i> = 10	<i>n</i> = 10
pH	5.5	5.7	5.6	5.7	5.6	5.8	5.7	5.8
(range)	(5.1–5.7)	(5.6–5.8)	(5.5–5.7)	(5.6–5.7)	(5.4–5.7)	(5.7–5.8)	(5.4–5.8)	(5.6–5.8)
Temp	17.5	17.8	17.7	17.7	18.4	18.9	17.9	18.2
(range)	(16–20)	(16.4–20.1)	(16.2–20.3)	(16.3–20.3)	(17–19.6)	(17.5–20)	(16–20.3)	(16.5–20.3)
*Cond	225.2	392	175.3333	382	230.6667	405	264.9	408.4
(range)	(148–373)	(336–435)	(170–186)	(338–415)	(206–276)	(359–436)	(162–416)	(342–452)
D.O. %	100	34	102	37	94	18	102	12
(range)	(78–109)	(10.4–43.2)	(99–105)	(13.1–52.7)	(80.5–101)	(8.3–28.1)	(98–111)	(7.8–23)
Redox Eh	509	482	499	491	483	428	485	423
(range)	(459–603)	(456.9–530)	(479–525)	(478.9–509)	(468–504)	(412.7–436)	(446–555)	(381–485)
Fe	0.0	0.1	0.0	0.1	0.7	0.1	0.0	0.3
(range)	0.0	(0–0.1)	(0–0.1)	(0–0.2)	(0–2)	(0.1–0.2)	(0–0.2)	(0.1–0.6)
Mn	0.1	0.1	0.0	0.1	0.1	3.5	0.2	5.8
(range)	(0–0.1)	(0.1–0.2)	0.0	(0–0.2)	(0–0.1)	(2.2–5.3)	(0–0.7)	(1–10.1)
Zn	15.6	53.9	14.8	<u>61.1</u>	22.8	<u>58.9</u>	24.6	52.0
(range)	(10.1–29.2)	(55.4–50)	(13.1–16.3)	(47.5–68.2)	(17.7–27)	(49.3–68.5)	(9.6–47.2)	(45.5–62.7)
Ca	2.4	11.8	2.0	13.7	4.7	15.7	5.7	13.6
(range)	(0–8)	(8–14)	(0–4)	(16–12)	(3–7)	(14–17)	(0–18)	(4–19)
Nitrate	1.6	1.4	0.6	1.9	1.1	0.1	0.7	0.0
(range)	(0.2–2.8)	(0.6–2.3)	(0–1.2)	(1–2.5)	(0.4–1.7)	(0–0.2)	(0–2.1)	(0–0.5)
Chloride	8.5	3.3	1.7	2.6	4.0	3.5	7.8	6.0
(range)	(2.4–23.5)	(2.6–4.8)	(1.27–2.48)	(1.4–3.4)	(1.6–6.4)	(1.1–5.5)	(1.5–27.6)	(0.7–17.5)
Sulphate	25.3	95.2	17.7	120.3	36.0	110.3	35.5	94.6
(range)	(8.5–64)	(121.9–47.7)	(8.8–35.2)	(90–145)	(19.3–52.9)	(66.6–147.7)	(7–115)	(46–138)
Na	2.2	4.8	3.0	4.7	5.3	14.3	7.3	8.8
(range)	(0–4)	(3–7)	(1–6)	(3–7)	(4–7)	(9–19)	(1–22)	(2–18)
K	1.2	1.0	0.0	0.7	0.3	1.0	2.8	0.7
(range)	(0–4)	1.0	0.0	(0–1)	(0–1)	1.0	(0–25)	(0–1)
DOC	2.5	3.1	1.9	3.1	2.6	4.3	2.6	3.6
(range)	(2.1–3.2)	(2.4–3.5)	(1.9–2)	(2.6–3.8)	(1.9–3)	(3.7–4.9)	(1.9–4.9)	(2.5–4.8)
TIC	0.8	1.2	0.6	1.1	0.8	2.8	0.7	2.5
(range)	(0.4–1.1)	(0.6–1.8)	(0.3–0.9)	(0.7–1.6)	(0.7–1.1)	(2.3–3.4)	(0.2–1.4)	(1.1–4.3)

‘n’ relates to number of samples taken at the end of a flood period. The ‘n’ varied between runs because certain runs had more flood periods than others over the treatment period

followed by the 3-week wet run ( $58.9 \pm 5.6$  mg l<sup>-1</sup>) (Table 2). For the 2nd mesocosm experiment, compared to the 1st mesocosm experiment, significantly higher concentrations of dissolved Zn were measured in pore water at the end of a flood at the bottom of the mesocosm ( $z = -1.96$ ,  $p = < 0.05$ ), average concentrations of Zn were approximately 2–3 times higher (Fig. 3b).

Trends in the release of dissolved Zn were found to vary for different wet and dry treatments at the bottom of the mesocosm. Spearman’s rho correlation analysis found that the relationships between dissolved Zn and other variables

(Fe, Mn, Ca, pH, sulphate and nitrate) were different for the longer or more frequent wet runs compared to the 3-week dry run. For the former, there was a significant positive relationship between dissolved Zn and dissolved Fe, Mn, sulphate, Ca ( $p = 0.01$ ) and pH ( $p = 0.05$ ) and a significant negative relationship between dissolved Zn and nitrate ( $p = 0.01$ ) (1st mesocosm experiment; see Online Resource 1 in the Electronic Supplementary Material). In the 2nd mesocosm experiment, there was a significant relationship between dissolved Zn and Mn ( $r = 0.928$ ,  $p = 0.01$ ,  $n = 6$ ) for the 3wwet run. Zinc displayed a *pulsed* pattern of release, where



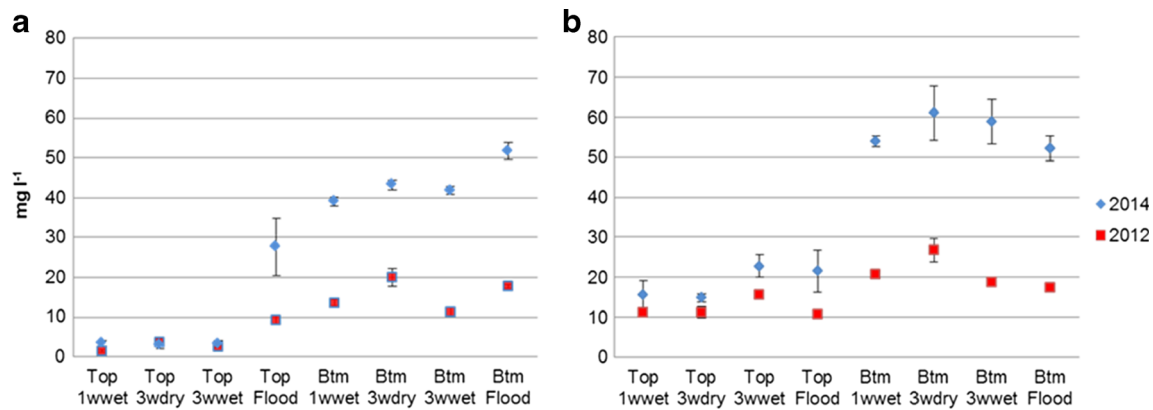


**Fig. 3** Average concentration ( $\text{mg l}^{-1}$ ) of Zn released at the start (a) and end (b) of a flood for mesocosm experiments in 2012 and 2014, by run, at the top and bottom. Bars represent standard error ( $n = \text{see Tables 1 and 2}$ )

concentrations increased between the start and end of a flooded period. In contrast, for the 3wdry run, there was a significant correlation with Zn and sulphate ( $r = 0.849$ ,  $p = 0.01$ ,  $n = 18$ ) and ( $r = 0.886$ ,  $p = 0.05$ ,  $n = 6$ ) for the 1st and 2nd mesocosm experiments, respectively, and a significant negative correlation between Zn and pH ( $r = -0.899$ ,  $p = 0.05$ ,  $n = 6$ ) (2nd mesocosm experiment), but no correlation between dissolved Zn and Mn or Fe. The 3-week dry run showed the highest average concentration of dissolved Zn released at the start of a flood (within 2–3 h), compared to the other variable runs (Fig. 3a). Moreover, simple regression analysis revealed that for the longer dry runs, particularly the 3-week dry and 2 week dry runs, dissolved Zn increased linearly over the treatment periods. The model accounted for >80% of the variation in dissolved Zn ( $p = 0.001$ ). These runs showed the highest week by week increase in dissolved Zn (1st mesocosm experiment; see Online Resource 2 in the Electronic Supplementary Material).

Calculations of saturation indices using PHREEQC for selected Zn mineral phases (bianchite  $\text{ZnSO}_4 \cdot 6\text{H}_2\text{O}$ ; zincite  $\text{ZnO}$ ;  $\text{ZnO(a)}$ ;  $\text{ZnSO}_4 \cdot \text{H}_2\text{O}$ ) showed they were all below saturation. Therefore, even at the  $>60 \text{ mg l}^{-1}$  dissolved Zn observed in pore water for some runs (Table 2), precipitation of Zn minerals could not have controlled dissolved Zn concentrations.

PCA was used to determine underlying factors influencing the mobilisation of Zn in pore waters at the bottom of the mesocosm (1st mesocosm experiment). Geochemical processes were likely to be different for the longer/more frequent wet runs where conditions could become more reducing, compared to runs with a longer dry period where soluble sulphate minerals could potentially build up. Therefore, the analysis was split into two parts: (a) longer or more frequent wet runs: 1wwet, 2wwet, 3wwet and field capacity (unsaturated run for comparison); (b) longer dryer runs, 2wdry, 3wdry and included both flood and field capacity for comparison.

For (a), two PCs had eigenvalues greater than '1': PC1 explained 63% and PC2 16% of the variance. The negative

factor loading for nitrate ( $-0.849$ ) and positive loading for Mn (0.881) and Fe (0.802) against PC1 indicate that this factor may represent redox potential (Fig. 4a). It is clear from the factor scores that pore water samples with longer 'wet' periods score highly against PC1 and pore water samples for the unsaturated field capacity run score negatively against PC1. If PC1 is related to redox potential, this could indicate that the wetter runs and field capacity run have very different redox potential conditions. A positive loading for Zn (0.86) against PC1 indicates that for the longer wetter runs, redox potential conditions may influence the mobilisation of Zn. For (b), two PCs had eigenvalues greater than '1': PC1 explained 58% and PC2 20% of the variance. As with part (a), the negative loading for nitrate ( $-0.75$ ) and positive loading for Mn (0.52) and Fe (0.46) against PC1 indicate PC1 may represent redox potential. The flood run samples scored highly against PC1 (Fig. 4b). However, the pore water samples with longer dry periods score negatively against PC1, indicating they have very different redox potential conditions to the flood samples and these samples scored highly against PC2. High loadings for Zn (0.919), sulphate (0.727) and calcium (0.915) were observed for PC2. This could indicate that for the longer dryer runs, high loadings associated with PC2 may influence the mobilisation of Zn.

### 3.2 Dissolved Zn and Mn, with depth in the sediment (DET)

For the 3wdry run, at the start of a flood, high concentrations of Zn can be seen at the bottom of the mesocosm (Fig. 5, 3wdry, week I). These results were similar to pore water findings, where high concentrations of Zn were released at the start of a flood following long dry antecedent conditions. This release was not apparent for the other runs at the start of a flood. For the 3wdry run, concentrations of dissolved Zn continue to increase at the top of the mesocosm over the submersed period (Fig. 5, 3wdry, week J). For the 1wwet, 3wwet and the flood runs Mn was mobilised over submersed periods

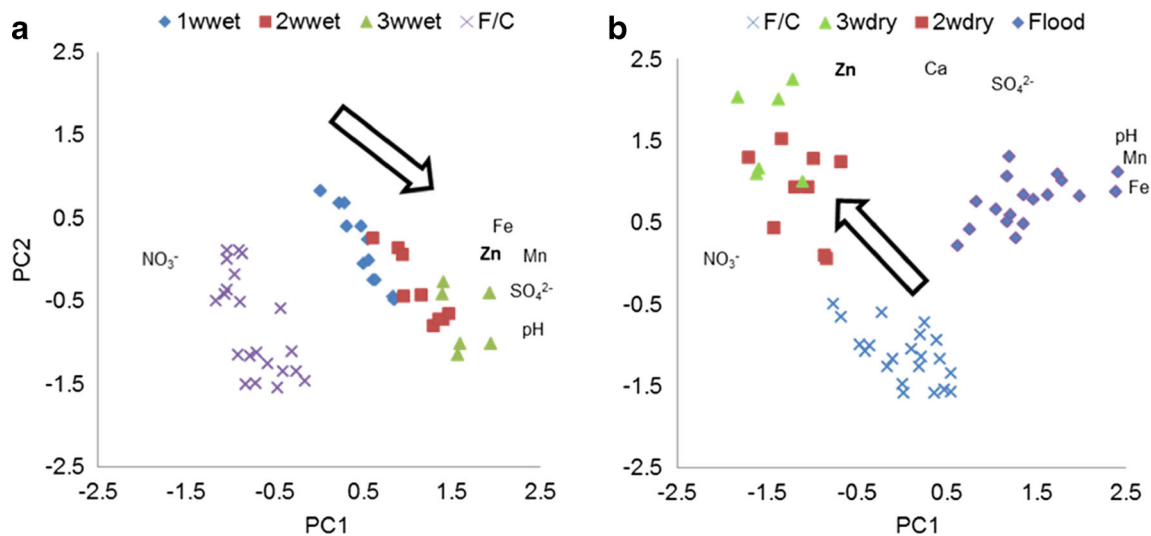


**Fig. 4** Principal component analysis showing the distribution of pore water chemical samples along the first two principal components (a) includes runs 1wwet, 2wwet, 3wwet and field capacity (F/C). The arrow shows the gradient of change as the treatments become wetter for

longer with Zn, Mn, Fe and  $\text{SO}_4^{2-}$  scoring highly against PC1 (b) includes runs 2wdry, 3wdry, flood and F/C. The arrow shows the gradient of change as the treatments become dryer for longer, with Zn,  $\text{SO}_4^{2-}$  and Ca scoring highly against PC2

(Fig. 5). Spearman's rho correlation analysis showed that for the 3wwet run, week I ( $r = 0.932$ ,  $p = 0.01$ ) and week L ( $r = 0.932$ ,  $p = 0.01$ ) and 1wwet run, week J ( $r = 0.807$ ,  $p = 0.01$ ), there was a significant positive relationship between dissolved Zn and Mn that was not apparent for the 3wdry run. The co-distribution of Zn and Mn observed in these figures indicates that the geochemical mechanisms of Zn and Mn release are linked. For the 3wwet run, Mn and Zn show similar patterns of mobilisation, with concentrations increasing at the bottom of the mesocosm. For the flood run by week J, Mn was mobilised throughout the depth profile and high concentrations of Zn were apparent throughout the depth profile too.

### 3.3 Environmental risk of contaminated sediments

Environmental quality standards (EQS) for Zn have recently been reviewed, and  $\text{EQS}_{\text{bioavailable}}$  concentrations have been proposed, taking into account the influence of Ca, DOC and pH and the natural background concentrations of the river following recommendations from the UK Technical Advisory Group (UKTAG). UK TAG however has recommended, in the short term, that the current standards remain for Zn as more data are required for the implementation of predicted no-effect concentrations (PNEC) (DEFRA 2014). The current EQS for Zn are based on water hardness ( $\text{CaCO}_3$ ), as there is a logarithmic linear relationship with water hardness and the toxicity of Zn to fish (DEFRA 2014).

In order to compare dissolved Zn concentrations observed in confined mesocosms with potential surface water concentrations in the riverbank environment, an estimated dilution calculation was carried out. Minimum and maximum Zn

concentrations were taken from Table 1 and Table 2 for the 1st and 2nd mesocosm experiments, and dilution was calculated as: 1 L of pore water exfiltrating from the riverbank and diluted with uncontaminated river water. Dimensions were based on the morphology of the river at the sample site (width 6 m  $\times$  depth 0.5 m  $\times$  length 0.25 m) =  $0.75 \text{ m}^3 \times 1000 = 750 \text{ L}$  water.

The results show (Table 3) that at the  $<50 \text{ mg l}^{-1} \text{CaCO}_3$  concentrations observed in pore and surface water of the current experiment, Zn concentrations for all runs (Table 3) exceed EQS and would be expected to cause adverse environmental effects and pose a significant environmental risk.

## 4 Discussion

Afon Ystwyth River has been identified as a top 30 priority mining 'impacted' water body in the western Wales river basin district (Environment Agency, 2012b), with large Zn loads in the river contributing to water quality objective failures in Wales (Natural Resources Wales, 2004). The present study has shown that the riverbank sediments are likely to be a major source of dissolved Zn to the river particularly in light of UK climate projections (UKCP09). Given the mildly acidic conditions of the mesocosm treatments and the high sorption edge for Zn (pH 5–6.5) (Smith 1999; Lee et al. 2002), it would be expected that some Zn would be in solution. However, the study found that altering the length of 'wet' or 'dry' period influenced the concentration of Zn released into pore water, and at the bottom of the mesocosm, the pore water results showed clear differences in the patterns of Zn release that

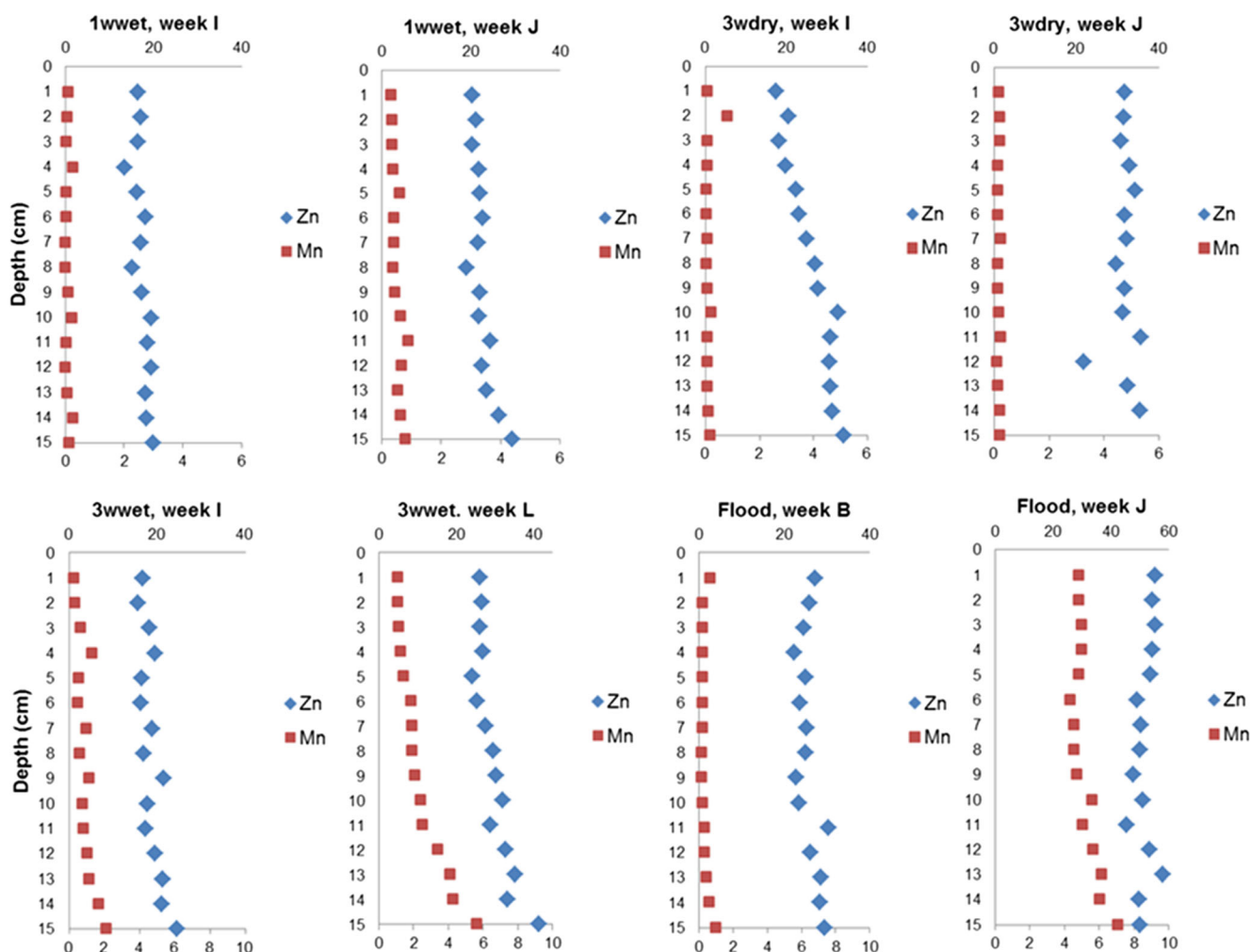


**Fig. 5** DET vertical depth profiles showing dissolved concentrations ( $\text{mg l}^{-1}$ ) of Mn and Zn for 1wwet, 3wdry, 3wwet and Flood runs. Two graphs for each run show concentrations ( $\text{mg l}^{-1}$ ) at the start and end of a wet period. Mn x-axis (bottom) and Zn x-axis (top). Note the differing

scales for each run. The weeks are labelled alphabetically and indicate the week of sampling (week b = second sample week, week I = 9th sample week, J = 10th sample week, L = 12th sample week)

indicated very different controlling geochemical mechanisms for longer wetter runs (1wwet, 2wwet and 3wwet) compared to longer dryer runs (2wdry, 3wdry).

#### 4.1 Impact of long wet (saturated) periods followed by shorter periods of exposure on the release of dissolved Zn

Results revealed a significant positive correlation between dissolved Zn and dissolved Fe and Mn and a significant negative relationship with nitrate, by the end of a flood period, for the longer wetter runs (1ww, 2ww, 3ww runs), indicating that mobilisation of Zn was linked to a fall in redox potential conditions. Dissolved oxygen and redox potential conditions were found to decline at the bottom of the mesocosm (2nd mesocosm experiment) with the lowest DO and redox potential measurements observed for the 3wwet and flood run. Zinc displayed a *pulsed* pattern of release, increasing in

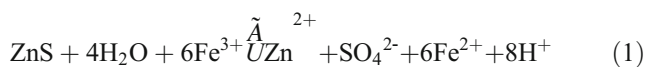
concentration between the start and end of a wet period. These results were found to concur with PCA analysis for the longer wet runs. Principal component 1 was found to represent redox potential conditions, and a gradient of change was observed for individual samples where those with longer wet periods scored more highly against PC1, along with

**Table 3** Comparison of diluted Zn min and max average concentrations for 1st and 2nd mesocosm experiments with EQS

Mesocosm experiment #	Zn $\text{mg l}^{-1}$	Zn after dilution $\mu\text{g l}^{-1}$
1st experiment (max)	26.8	35.7
1st experiment (min)	7.7	10.3
2nd experiment (max)	61.1	81.5
2nd experiment (min)	14.8	19.7

EQS for *total concentration of Zn* for the protection of surface water is  $8 \mu\text{g l}^{-1}$  (annual average value) at  $0\text{--}50 \text{ mg l}^{-1} \text{ CaCO}_3$

dissolved Zn. It is possible that the dissimilatory reduction of Fe and/or Mn (hydr)oxides occurred in response to a fall in redox potential conditions due to prolonged flooding (Lynch et al. 2014). However, although dissolved Fe was measured in pore water, redox potential conditions did not decline low enough for the reductive dissolution of Fe (hydr)oxide (<300 mV, pH 5) (Gotoh and Patrick 1974; Emerson et al. 1979). Several possible geochemical mechanisms for the release of dissolved Fe into pore water are: the oxidation of impure sphalerite (Heidel et al. 2013), oxidation of sphalerite coupled to the reduction of ferric Fe (Eq. 1) (Hofmann and Schuwirth 2008), or the dissolution of soluble Fe sulphate minerals such as melanterite ( $\text{Fe}_2\text{SO}_4 \cdot 7\text{H}_2\text{O}$ ) (Alastuey et al. 1999; Buckby et al. 2003; Nordstrom 2009).



In contrast to Fe, Mn solubility is more sensitive to a fall in redox potential conditions (Lee et al. 2002; Patrick and Henderson 1981; Patrick and Delaune 1972), and visual inspection of simplified Pourbaix diagrams for Mn (Najafpour et al. 2014; Fruh 2006) indicates reductive dissolution of Mn hydroxides would be likely to occur over the longer flooded periods at the Eh and pH measured in pore water, with the potential to release high concentrations of Zn into pore water. Diffusional equilibration in thin film analysis has been used to measure the co-distribution of redox-sensitive solutes and contaminant trace metals under low redox potential conditions, with depth in ‘soft’ fine grained sediment (Tankere-Muller et al. 2007; Gao et al. 2006). The present study incorporated a temporal element and measured the mechanistic interactions of redox-sensitive solutes and dissolved Zn, at the *start* and *end* of a flood period. Results show a significant correlation between Zn and Mn depth profiles for the 1wwet and 3wwet runs. Higher concentrations of Zn and Mn were observed at the end of a flood, compared to the start at the bottom of the mesocosm (depth 5–15 cm), particularly for the 3wwet run. The occurrence of dissolved Mn at similar depths >10 cm (Ullah et al. 2012; Byrne et al. 2014) has been observed in DET studies of coarse-grained sediment of the River Leith. In the current study, the medium to low DOC levels seemed sufficient to promote reduction of Mn, particularly over the longer flood periods (3wwet, flood). In the field, the introduction of DOC through carbon-rich downwelling surface water and lateral subsurface flows was reported as a key driver of microbial reduction in the shallow sandy sediments (Byrne et al. 2013; Byrne et al. 2014). At mining-impacted sites, additional sources of DOC introduced in this fashion could promote the microbial oxidation of labile organic carbon and accelerate the reduction of Mn (hydr)oxides, resulting in the release of any partitioned Zn into pore water over shorter flood periods (Patrick and Delaune 1972). Data

from a parallel study also showed that sediment with a higher concentration of labile (easily reducible) Mn (hydr)oxides (partitioned with Zn) leads to higher releases of Zn over prolonged flood periods (see section 4.3, Lynch et al. unpublished). Lower concentrations of dissolved Mn and Zn observed at the start of a flood in the current study indicated that on draining of the sediment and exposure to atmospheric conditions, the oxidation of reduced Mn, precipitation of Mn (hydr)oxides and sorption of Zn were a controlling mechanism. Manganese (hydr)oxide minerals such as manganite  $\text{MnO}(\text{OH})$  have a low (<pH 4) point of zero charge (Clarke et al. 2012), and the resulting negative surface charge on the surface of Mn hydroxides at the pH of the pore water in the current study would encourage sorption of cations such as Zn (Appelo and Postma 2010). Studies on mining contaminated soil in Ronneburg, Germany found at low pH (pH 4.7–5.1) that the formation of Mn oxide layers efficiently immobilised Zn (Mayanna et al. 2015). Furthermore, laboratory experiments on streambed sediments show that in the hyporheic zone (a dynamic redox environment), the ongoing formation of Mn oxides enhanced dissolved Zn uptake and Zn uptake increased with Mn oxide concentration (Fuller and Harvey 2000). Indeed, a microcosm study of Nile Delta wetland soil used for agricultural purposes found that, on oxidation, Fe–Mn (hydr)oxides acted as important binding agents for dissolved Zn through various sorption mechanisms, although this process was highly pH dependent (Shaheen et al. 2016). In this way, Mn hydroxides could partially control the release of Zn at the start of a flood, and while conditions remain highly oxidic, however, these minerals may quickly become a source of Zn contamination during prolonged flooding (Charlatchka and Cambier 2000; Lesven et al. 2010). The effects of prolonged hydrological saturation were apparent through DET analysis of the flood run that revealed high concentrations of Zn and Mn throughout the vertical concentration profile by week J. During the constant flood run, Mn (hydr)oxides may have provided a source of Zn contamination due to reductive dissolution processes; however with no drainage period for Mn (hydr)oxides to attenuate Zn, average dissolved Zn concentrations rose to >60 mg l<sup>-1</sup>. Calculations of saturation indices showed that all Zn sulphate minerals remained under-saturated, indicating the solubility of these minerals would have no control over dissolved Zn concentrations and therefore high concentrations of dissolved Zn would continue to be released into pore water unchecked.

Climate predictions indicate an increase in the amount and intensity of rainfall, particularly in winter. As a result, river flooding would be expected to increase in frequency and duration. The resulting changes in river stage would sequentially expose and submerge the riverbank and that could set up a cycle of precipitation of Fe/Mn (hydr)oxides and sorption of Zn during exposed oxidised periods, followed by reductive dissolution of Fe/Mn (hydr)oxides and release of Zn during



prolonged flooding. Our results indicate that the frequency and magnitude of Zn pollution events could increase, particularly over the longer flood periods expected in the winter months.

#### 4.2 Impact of long dry antecedent periods followed by shorter periods of submersion on the release of dissolved Zn

The highest average concentrations of dissolved Zn were observed at the start (within 2–3 h) and end of a flood period for the 3wdry run compared to other variable runs. For runs with longer dry periods, contrary to the longer wet runs, pore water and PCA analysis revealed that releases of dissolved Zn were linked to more oxidising conditions, a fall in pH (2nd mesocosm experiment) and releases of sulphate, calcium only, and not Fe and Mn. Previous mesocosm studies have observed a release of Zn and Ca over flooded periods for sequences with long dry periods (Du Laing et al. 2007), possibly as a result of carbonate dissolution following a fall in pH. However, in the current study, carbonates in the sediment were below detection and results from piper analysis (not included in this study) indicated that the water samples were typical of mine drainage (Ca-sulphate) water type. Therefore, the mobilisation of Ca is more likely to be related to the dissolution of gypsum ( $\text{CaSO}_4 \cdot 2\text{H}_2\text{O}$ ) often present in mining impacted catchments (Younger 1998b; Harris et al. 2003; Kuechler et al. 2004). DET analysis of the 3wdry run also revealed, in contrast to the wetter runs, very little dissolved Mn was mobilised. Instead, an increase in dissolved Zn was observed at the *start* of a flood, with depth (>5 cm) (3wdry, week I) that was not apparent for the other runs. For this run, dissolved Zn concentrations increased towards the surface (<10 cm) over the flood period (3wdry, week J). The greatest increase in dissolved Zn concentration is closest to the sediment/water interface. It is possible that over prolonged dry periods, the evaporation of pore water and chemical saturation of solutes could have promoted the formation of soluble metal sulphate minerals (Alastuey et al. 1999; Harris et al. 2003; Buckby et al. 2003; Nordstrom 2009). The dissolution of these salts on first flood wetting could account for the high concentrations of dissolved Zn released into pore water at the start of a flood. Over flooded periods, redox potential conditions and dissolved oxygen were found to remain high even at the bottom of the mesocosms and therefore the observed increase in dissolved Zn concentrations could be due to the oxidation of Zn sulphide minerals under more oxic conditions particularly towards the sediment/water interface (Wragg and Palumbo-Roe 2011). Similarly, Shaheen et al. (2014) observed an increase in dissolved Zn at the start of a flood under high redox-potential conditions, possibly due to oxidation of Zn associated sulphide minerals. Contrary to the 3wwet run, it is unlikely that the oxidation of previously reduced Mn

(hydr)oxide minerals would have provided a solubility control over the release of dissolved Zn concentrations, particularly at the start of a flood. Therefore, the sediment could, within hours, become a significant source of Zn contamination following prolonged dry periods due to formation of soluble sulphate minerals (Buckby et al. 2003; Nordstrom 2009) and the dissolution of these salts on flooding. Studies have described a ‘spike’ in trace metal concentrations on the rising limb of river discharge during storm events due to the dissolution and ‘flushing’ of salts back into river channels following long dry antecedent periods (Nordstrom 2011). Byrne et al. (2013) report a similar high flux of trace metals during storm events linked to extended dry antecedent periods. These authors noted the ‘immediacy’ of initial contaminant trace metal peaks indicated the dissolution of soluble metal sulphate minerals on the surface of mine spoil was the principle source of contamination. It is therefore likely, considering the speed dissolved Zn was released into pore water, that soluble metal salts built up over long dry periods and were quickly dissolved on wetting releasing a spike of Zn into pore water. Any fall in pH would be poorly buffered in the low alkalinity waters and could serve to promote dissolved Zn release further. This raises serious concerns in light of UK climate projections that indicate a shift towards aridity particularly in the summer months. These changes would be expected to increase the length of antecedent dry period along riverbanks, and as a result, acute releases of dissolved Zn to impacted river systems could increase in magnitude and/or become more frequent.

#### 4.3 Environmental risk of the sediment

Releases of dissolved Zn were found to exceed EQS for all runs. Therefore, it is likely that the river would fail EU WFD requirements based on inputs of dissolved Zn from riverbank sediment alone without taking into account any other point source of pollution.

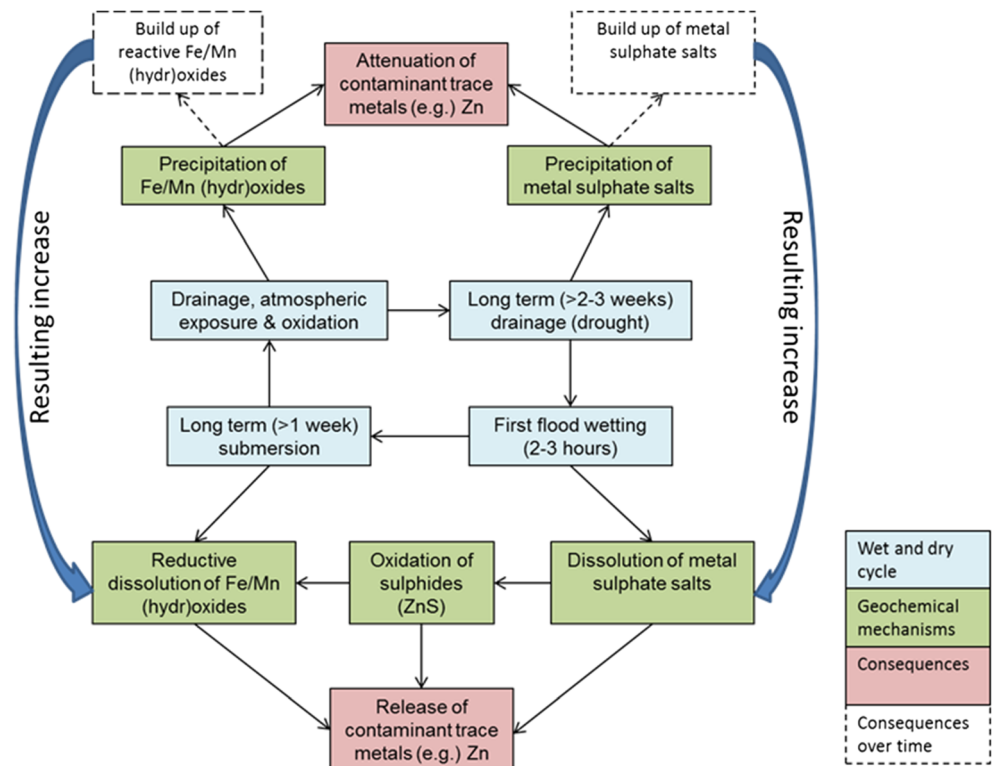
Analysis (not included in this study) indicated Zn was partitioned with a higher labile Mn content in the sediment collected for the 2nd mesocosm experiment. That seemed to result in higher concentrations of dissolved Zn released into pore water for the 2nd mesocosm experiment (unpublished Lynch et al.). This is a concern as the sediment sample location for this experiment was close to the active channel and likely to experience the perturbations discussed in this study due to changes in river stage.

#### 4.4 Conceptual model for Zn cycling

The results from the current study were used to create a conceptual model that summarises the environmental perturbations and key geochemical mechanisms controlling the cycling of Zn (Fig. 6).



**Fig. 6** Conceptual model of Zn cycling showing the hydrological stages in wet and dry cycle (blue) that result in ‘key’ geochemical mechanisms (green) responsible for controlling Zn attenuation and release (pink)



The right side of Fig. 6 is representative of sequences with longer dry periods, where the ‘key’ geochemical control mechanisms are precipitation of Zn sulphate salts in response to long-term drainage, leading to the attenuation of Zn, followed by releases of dissolved Zn on first flood wetting. The left side represents sequences with long (>1 week) wet/flood periods, where the ‘key’ geochemical control mechanisms are (i) the reductive dissolution of Fe/Mn (hydr)oxides and release of partitioned Zn and (ii) the precipitation of Fe/Mn (hydr)oxides on exposure to atmospheric conditions after long-term flooding and attenuation of Zn. The model also incorporates an increase in reactivity of sediment over time. A week by week increase in dissolved Zn was observed for the longer dry runs (2wdry, 3wdry) that indicated a build-up of sulphate salts (1st mesocosm experiment). Furthermore, studies show that freshly precipitated Fe (hydr)oxide minerals can be reduced more quickly (Lovley and Phillips 1987) at a higher redox potential (Du Laing et al. 2009) and it is possible that prolonged sequences of flooding followed by exposure could result in buildup of reactive Fe/Mn hydroxides. A buildup of more labile Fe hydroxide (and partitioned Zn) in the sediment has been observed in response to wet and dry sequences in a parallel study (unpublished Lynch et al.). At the bottom of the model, the wet period extends from ‘first flood wetting’ to ‘long-term submersion’ (blue)

and the key geochemical processes (green) show a shift from more ‘acute’ inputs of Zn (dissolution of metal sulphate salts) to become more ‘chronic’ (oxidation of sulphides and reductive dissolution of Fe/Mn).

The conceptual model highlights the links between hydrological perturbation and key controlling geochemical mechanisms. It therefore could be used as a guide to understand the processes responsible for dissolved Zn releases in the field and a tool to predict the consequences of future UK climate projections (UKCP09).

## 5 Conclusions

The Cwmystwyth mine site is one of the main sources of pollution to the Afon Ystwyth River (Dyfed Archaeological Trust 2014). Flow data for the Cwmystwyth site (Centre for Ecology and Hydrology 2015) indicate that prolonged (>1 week) periods of high flow and low flow (well above and below the mean) are common, and therefore, it is likely that the perturbations discussed in this study occur in the riverbank sediment resulting in releases of dissolved Zn. The mineralogy at the Cwmystwyth site is common to many mining impacted sites, and therefore, it is likely that the geochemical processes observed in the current study would be widespread. Previous field and mesocosm studies have observed similar patterns of trace metals release in response to storm

events. This study however has directly linked patterns of Zn release to alternating periods of submersion and exposure for different durations and frequencies. Considering future climate change projections (UKCP09), the results indicate that if the predicted increases in aridity come about in summer months, resulting in a fall in river stage and exposure of river bank sediment, the saturation of Zn sulphate salts and ‘flushing’ of contaminants on first flood wetting may be a key geochemical mechanism resulting in ‘acute’ ecotoxic releases of Zn. Furthermore, if predicted, rainfall and peak river flow increases occur during winter months, then a rise in river stage followed by inundation of river bank sediment could result in reductive dissolution of Mn (hydr)oxides and ‘chronic’ releases of partitioned Zn over prolonged flooded periods. Where these floods are interspersed with shorter periods of drainage, precipitation of Mn (hydr)oxides and sorption reactions may attenuate Zn, but only in the short term. Taking into account the seasonal changes predicted in future UK climate projections (UKCP09), it is possible we may see a seasonal shift in the type (acute/chronic) and/or location of Zn contamination to river systems. The conceptual model of Zn cycling provides a guide as to the key geochemical mechanisms controlling these releases, information that could help during early stages of catchment wide scoping studies to identify the sources of diffuse pollution (Environment Agency 2012c). Further support of these findings may be gained through long-term field studies at severely contaminated metal mining sites that monitor dissolved Zn and Mn concentrations in river surface and pore water during real flood waves.

There are known point sources of pollution from several adits at the Cwmystwyth site (Dyfed Archaeological Trust 2014). However, our results indicate that remediation of point sources alone may not reduce Zn to within EQS standards and inputs from riverbank sediment would need to be taken into account. Furthermore, our findings show that pollution may be transient in nature, the frequency and magnitude of Zn contamination relating to temporal and spatial factors linked to alternate wetting and drying of sediment. In light of the above statement, it is therefore essential to locate the precise sources of pollution in the field over a range of hydrological conditions (Environment agency 2012c), taking into account the complex hydrology of mining sites so that an informed management decision can be made regarding remediation.

**Acknowledgments** This study was funded by Natural Environment Research Council.

Thanks to Professor Dave Polya, Alastair Bewsher and Paul Lythgoe, University of Manchester, School of Earth Atmospheric and Environmental Sciences, for carrying out anion analysis of samples using their Ion Chromatography (Dionex ICS2000) machine during the second mesocosm run.

**Open Access** This article is distributed under the terms of the Creative Commons Attribution 4.0 International License (<http://creativecommons.org/licenses/by/4.0/>), which permits unrestricted use, distribution, and reproduction in any medium, provided you give appropriate credit to the original author(s) and the source, provide a link to the Creative Commons license, and indicate if changes were made.

## References

- Alastuey A, Garcia-Sanchez A, Lopez F, Querol X (1999) Evolution of pyrite mud weathering and mobility of heavy metals in the Guadamar valley after the Aznalcollar spill, South-West Spain. *Sci Total Environ* 242:41–55
- Appelo CAJ, Postma D (2010) *Geochemistry, groundwater and pollution*, 3rd edn. A.A. Balkema Publishers, Leiden, The Netherlands
- Bick DE (1976) The old metal mines of mid-Wales. Part 1 Cardiganshire—south of Devil’s bridge. The Pound House, Newent, Glos
- Bird G, Brewer PA, Macklin MG (2010) Management of the Danube drainage basin: implications of contaminant-metal dispersal for the implementation of the EU water framework directive. *Intl J River Basin Management* 8:63–78
- British Geological Survey (2007) *British regional geology: Wales*. British Geological Survey, Nottingham
- Buckby T, Black S, Coleman ML, Hodson ME (2003) Fe-sulphate-rich evaporative mineral precipitates from the Rio Tinto, Southwest Spain. *Mineral Mag* 67:263–278
- Byrne P, Reid I, Wood PJ (2013) Stormflow hydrochemistry of a river draining an abandoned metal mine: the Afon Twymyn, Central Wales. *Environ Monit Assess* 185:2817–2832
- Byrne P, Zhang H, Ullah S, Binley A, Heathwaite AL, Heppell CM, Lansdown K, Timmer M (2014) Diffusive equilibrium in thin films provides evidence of suppression of hyporheic exchange and large-scale nitrate transformation in a groundwater-fed river. *Hydrol Process* 6:1385–1396
- Carroll SA, O’Day PA, Piechowski M (1998) Rock-water interactions controlling zinc, cadmium, and lead concentrations in surface waters and sediments, US tri-state mining district. 2. Geochemical interpretation. *Environ Sci Technol* 32:956–965
- Centre for Ecology and Hydrology (2015) National river flow archive. <http://www.ceh.ac.uk/data/nrfa/data/station.html?63004>. Accessed 101015
- Charlatchka R, Cambier P (2000) Influence of reducing conditions on solubility of trace metals in contaminated soils. *Water Air Soil Pollut* 118:143–167
- Clarke C, Tournay J, Johnson K (2012) Oxidation of anthracene using waste Mn oxide minerals: the importance of wetting and drying sequences. *J Hazard Mater* 205–206:126–130
- Collins A, Ohandja D, Hoare D, Voulvoulis N (2012) Implementing the water framework directive: a transition from established monitoring networks in England and Wales. *Environ Sci Pol* 17:49–61
- Gao Y, Leermakers M, Gabelle C, Divis P, Billon G, Ouddane B, Fischer J-C, Wartel M, Baeyens W (2006) High-resolution profiles of trace metals in the pore waters of riverine sediment assessed by DET and DGT. *Sci Total Environ* 362:266–277
- DEFRA (2012a) Climate change risk assessment for the floods and coastal erosion sector project code GA0204. Crown. <http://randd.defra.gov.uk/Default.aspx?Module=More&Location=None&ProjectID=15747>. Accessed 10102014
- DEFRA (2012b) Climate change risk assessment for the water sector. project code GA0204. Crown. <http://randd.defra.gov.uk/Default.aspx?Module=More&Location=None&ProjectID=15747>. Accessed 10102014

- DEFRA (2014) Water framework directive implementation in England and Wales: new and updated standards to protect the water environment. DEFRA, Wales
- Dennis IA, Macklin MG, Coulthard TJ, Brewer PA (2003) The impact of the October–November 2000 floods on contaminant metal dispersal in the river Swale catchment, North Yorkshire. *Hydrol Process* 17: 1641–1657
- Dennis IA, Coulthard TJ, Brewer P, Macklin MG (2009) The role of floodplains in attenuating contaminated sediment fluxes in formerly mined drainage basins. *Earth Surf Proc Land* 34:453–466
- Desbarats AJ, Dirom GC (2007) Temporal variations in the chemistry of circum-neutral drainage from the 10-level portal, Myra mine, Vancouver island, British Columbia. *Appl Geochem* 22:415–435
- Du Laing G, Vanthuyne DR, Vandecasteele B, Tack FM, Verloo MG (2007) Influence of hydrological regime on pore water metal concentrations in a contaminated sediment-derived soil. *Environ Pollut* 147:615–625
- Du Laing G, Rinklebe J, Vandecasteele B, Meers E, Tack FMG (2009) Trace metal behaviour in estuarine and riverine floodplain soils and sediments: a review. *Sci Total Environ* 407:3972–3985
- Dyfed Archaeological Trust (2014) Cwmystwyth mines, Ceredigion: management and protection plan. Dyfed Archaeological Trust, Wales
- Emerson S, Cranston RE, Liss PS (1979) Redox species in a reducing fjord: equilibrium and kinetic considerations deep sea research part A. *Oceanographic Research Papers* 26A:859–878
- Environment Agency (2008a) Abandoned mines and the water environment. Environment Agency, Bristol
- Environment Agency (2008b) Assessment of metal mining contaminated river sediments in England and Wales. Environment Agency, Bristol
- Environment Agency (2012a) Prioritisation of abandoned non-coal mine impacts on the environment. SC030136/R2 the national picture. Environment Agency, Bristol
- Environment Agency (2012b) Prioritisation of abandoned non-coal mine impacts on the environment. SC030136/R6 the western Wales river basin district. Environment Agency, Bristol
- Environment Agency (2012c) Prioritisation of abandoned non-coal mine impacts on the environment. SC030136/R12 future management of abandoned non-coal mine water discharges. Environment Agency, Bristol
- Field A (2009) *Discovering statistics using SPSS*, 3rd edn. SAGE Publications Ltd, London
- Foulds SA, Brewer PA, Macklin MG, Haresign W, Bretson RE, Rassner SME (2014) Flood-related contamination in catchments affected by historical metal mining: an unexpected and emerging hazard of climate change. *Sci Total Environ*: 476–477
- Fruh A (2006) Pourbaix diagram for manganese;  $c(\text{Mn}) = 1 \text{ mol/l}$ ,  $T = 25^\circ\text{C}$ . Western Oregon University. [https://www.commons.wikimedia.org/wiki/File:Pourbaix\\_diagram\\_for\\_Manganese.svg](https://www.commons.wikimedia.org/wiki/File:Pourbaix_diagram_for_Manganese.svg). Accessed 18/09/2015
- Fuge R, Laidlaw IMS, Perkins WT, Rogers KP (1991) The influence of acidic mine and spoil drainage on water quality in the mid-Wales area. *Environ Geochem Hlth* 13:70–75
- Fuller CC, Harvey JW (2000) Reactive uptake of trace metals in the hyporheic zone of a mining-contaminated stream, Pinal Creek Arizona. *Environ Sci Technol* 34:1150–1155
- Gerhardt A, Janssens De Bisthoven L, Soares AMVM (2004) Macroinvertebrate response to acid mine drainage: community metrics and on-line behavioural toxicity bioassay. *Environ Pollut* 130: 263–274
- Gotoh S, Patrick WH (1974) Transformation of iron in a waterlogged soil as influenced by redox potential and pH. *Soil Sci Soc Am J* 38:66–71
- Gozzard E, Mayes WM, Potter HA, Jarvis AP (2011) Seasonal and spatial variation of diffuse (non-point) source zinc pollution in a historically metal mined river catchment, UK. *Environ Pollut* 159:3113–3122
- Harris DL, Lottermoser BG, Duchesne J (2003) Ephemeral acid mine drainage at the Montalbion silver mine, North Queensland Aust. *J Earth Sci* 50:797–809
- Heidel C, Tichomirowa M, Junghans M (2013) Oxygen and sulfur isotope investigations of the oxidation of sulfide mixtures containing pyrite, galena, and sphalerite. *Chem Geol* 342:29–43
- Hofmann T, Schuwirth N (2008) Zn and Pb release of sphalerite (ZnS)-bearing mine waste tailings. *J Soils Sediments* 8:433–441
- Hughes SJS (1981) The Cwmystwyth mines vol 17. British mining no. 17. Northern Mine Research Society
- Kuechler R, Klaus N, Zorn T (2004) Investigation of gypsum dissolution under saturated and unsaturated water conditions. *Ecol Model* 176:1–14
- Laine DM (1999) The treatment of pumped minewater at Wooley colliery, West Yorkshire. *JCIWEM* 13:127–130
- Lee G, Bigham JM, Faure G (2002) Removal of trace metals by coprecipitation with Fe, Al and Mn from natural waters contaminated with acid mine drainage in the Ducktown mining district, Tennessee. *Appl Geochem* 17:569–581
- Lesven L, Lourino-Cabana B, Billon G, Recourt P, Ouddane B, Mikkelsen O, Boughriet A (2010) On metal diagenesis in contaminated sediments of the Deule river (northern France). *Appl Geochem* 25:1361–1373
- Lovley DR, Phillips EJP (1987) Competitive mechanisms for inhibition of sulfate reduction and methane production in the zone of ferric iron reduction in sediments. *Appl Environ Microb* 53:2636–2641
- Lynch SFL, Batty LC, Byrne P (2014) Environmental risk of metal mining contaminated river bank sediment at redox-transitional zones. *Minerals* 4:52–73
- Macklin MG, Brewer PA, Hudson-Edwards KA, Bird G, Coulthard TJ, Dennis IA, Lechler PJ, Miller JR, Turner JN (2006) A geomorphological approach to the management of rivers contaminated by metal mining. *Geomorphology* 79:423–447
- Mayanna S, Peacock CL, Schaffner F, Grawunder A, Merten D, Kothe E, Buchel G (2015) Biogenic precipitation of manganese oxides and enrichment of heavy metals at acidic soil pH. *Chem Geol* 402:6–17
- Mayes WM, Potter HAB, Jarvis AP (2013) Riverine flux of metals from historically mined orefields in England and Wales. *Water Air Soil Pollut* 224:1425. doi:10.1007/s11270-012-1425-9
- MET Office (2016) Climate. MET office. <http://www.metoffice.gov.uk/public/weather/climate/gcm3c7x2r>. Accessed 17/08/16
- Meybeck M (1982) Carbon, nitrogen and phosphorus transport by world rivers. *Am J Sci* 282:401–450
- Montserrat AM (2010) Environmental impact of mine drainage and its treatment on aquatic communities. University of Birmingham, Dissertation
- Najafpour MM, Hotynska M, Shamkhili AN, Kazemi SH, Hillier W, Amini E, Ghaemmaghami M, Sedigh DH, Moghaddam AN, Mohamadi R, Zaynalpoor S, Beckmann K (2014) The role of nano-sized manganese oxides in the oxygen-evolution reactions by manganese complexes: towards a complete picture. *Dalton T* 43:13122–13135
- Wales NR (2004) A metal mines strategy for Wales. Natural Resources Wales, Wales
- Neal C, Reynolds B, Neal M, Pugh B, Hill L, Wickham H (2001) Long-term changes in the water quality of rainfall, cloud water and stream water for moorland, forested and clear-felled catchments at Plynlimon, mid-Wales. *Hydrol Earth Syst Sc* 5:459–476
- Nordstrom DK (2009) Acid rock drainage and climate change. *J Geochem Explor* 100:97–104
- Nordstrom DK (2011) Hydrogeochemical processes governing the origin, transport and fate of major and trace elements from mine wastes and mineralized rock to surface waters. *Appl Geochem* 26:1777–1791

- Patrick WH, Delaune RD (1972) Characterization of oxidized and reduced zones in flooded soil. *Soil Sci Soc Am J* 36:573
- Patrick WH, Henderson RE (1981) Reduction and reoxidation cycles of manganese and iron in flooded soil and in water solution. *Soil Sci Soc Am J* 45:855–859
- Shaheen SM, Rinklebe J, Rupp H, Meissner R (2014) Temporal dynamics of pore water concentrations of Cd, Co, Cu, Ni and Zn and their controlling factors in a contaminated floodplain soil assessed by undisturbed groundwater lysimeters. *Environ Pollut* 191:223–231. doi:10.1016/j.envpol.2014.04.035
- Shaheen SM, Frohne T, White RW, Delaune RD, Rinklebe J (2016) Redox-induced mobilization of copper, selenium, and zinc in deltaic soils originating from Mississippi (U.S.a.) and Nile (Egypt) river deltas: a better understanding of biogeochemical processes for safe environmental management. *J Environ Manag* 186(Part 2):131–140
- Shimadzu Scientific Instruments (2014) List of Shimadzu application notes. <https://www.ssi.shimadzu.com/literature/litSearchResults.cfm>. Accessed 01052014
- Smith K (1999) Metal sorption on mineral surfaces: an overview with examples relating to mineral deposits vol 6A. The environmental geochemistry of mineral deposits part a: processes, techniques and health issues. Society of Economic Geologists, Colorado, USA
- Tankere-Muller S, Zhang H, Davison W, Finke N, Larsen O, Stahl H, Glud RN (2007) Fine scale remobilisation of Fe, Mn, Co, Ni, Cu and Cd in contaminated marine sediment. *Mar Chem* 106:192–207
- UK Technical Advisory Group on the Water Framework Directive (2008) Proposals for environmental quality standards for annex VIII substances. UK Technical Advisory Group on the Water Framework Directive
- Ullah S, Zhang H, Heathwaite AL, Binley A, Lansdown K, Heppell K, Trimmer M (2012) In situ measurement of redox sensitive solutes at high spatial resolution in a riverbed using diffusive equilibrium in thin films (DET). *Ecol Eng* 49:18–26
- Ullah S, Zhang H, Heathwaite AL, Heppell C, Lansdown K, Binley A, Trimmer M (2014) Influence of emergent vegetation on nitrate cycling in sediments of a groundwater-fed river. *Biogeochemistry* 118:121–134
- United States Environmental Protection Agency (1992) Standard operating procedure for GLNPO total alkalinity titration. United States Environmental Protection Agency. USA, Chicago
- Wragg J, Palumbo-Roe B (2011) Contaminant mobility as a result of sediment inundation: literature review and laboratory scale pilot study on mining contaminated sediments. British Geological Survey Open Report, 90 pp (OR/11/051)
- Young EA, Dawson EJ, Macklin MG, Zhao Y (2007) Mobilisation and deposition of metal contaminated sediments in the river Swale, North Yorkshire, UK. Paper presented at the European Geosciences Union
- Younger PL (1998a) Adit hydrology in the long-term: observations from the Pb-Zn mines of northern England. Paper presented at the IMWA Symposium Johannesburg, South Africa
- Younger PL (1998b) Coalfield abandonment: geochemical processes and hydrochemical products. In: Nicholson K (ed) *Energy and the Environment: Geochemistry of fossil, nuclear and renewable resources* MacGregor Science, pp 1–29
- Younger PL (2000) Predicting temporal changes in total iron concentrations in groundwaters flowing from abandoned deep mines: a first approximation. *J Contam Hydrol* 44:47–69
- Zhang X, Yang L, Li Y, Li H, Wang W, Ye B (2012) Impacts of lead/zinc mining and smelting on the environment and human health in China. *Environ Monit Assess* 184:2261–2273